Nuclear Energy Levels of Na^{24} in the Region from 350 to 630 kev*†

CARL T. HIBDON
Argonne National Laboratory, Argonne, Illinois
(Received May 9, 1960)

The neutron cross-section data from 350 to 630 kev show 71 peaks, consisting of a relatively small number of large peaks and many small peaks. Each of the previously known large peaks was resolved into two or more components. The analyses show a few s-wave levels, a small number of p-wave levels, and a large number of d- and f-wave levels. For all of the levels of Na^{24} up to 630 kev, a plot of the number of levels having energies $\leq E_n$ as a function of the neutron energy E_n shows an essentially linear distribution. The distribution of the angular momenta is in agreement with the theoretical distribution for a value of $\sigma=1.8$. The level spacings appear to agree with an exponential distribution. For the reduced neutron widths, the results appear to agree equally well with the exponential and Porter-Thomas distributions. The strength function obtained from the reduced widths has an average value of 0.045 for both values of J for $l=0$ and an average value of 0.37 for all values of J for $l=1$. For higher values of l, the strength function is too large. An expression developed for the distribution of the levels above the ground state tends to agree with the data for a value of 0.50 Mev for δ, the average level spacing of the nucleons in the nucleus.

1. INTRODUCTION

THE virtual nuclear energy levels of Na^{24} have been investigated up to 630 kev by the $Na^{23}(n,n)$ process. Because of the profusion of levels observed the paper was divided into parts. Only the levels in the region from about 1–350 kev were discussed in the first paper.[1] Previously, Stelson and Preston[2] studied the level structure of Na^{24} from about 0.12–1 Mev by use of wide neutron energy spreads and found a number of large peaks. As reported in the first paper on the present investigation, each of these large peaks below 350 kev could be resolved into two or more components and many narrower peaks were found between these large ones. The present paper extends this study over the range from 350–630 kev. All energies in this report are energies of the incident neutrons in the laboratory system unless otherwise noted.

2. EXPERIMENTAL METHOD

The experimental techniques and procedures are the same as those previously used and described in detail in other publications.[1,3,4] As before, the $Li^7(p,n)$ reaction was used to produce nearly monoenergetic neutrons of variable energy. Protons of well-defined energy were produced by the Argonne Van de Graaff accelerator. The same samples of high-purity sodium metal used for measurements up to 350 kev[1] were also used for the present measurements. While the resonances below 350 kev[1] were under investigation, the flat-detection measurements[1] were made up to about 500 kev by use of neutrons emitted at an angle of 120° with respect to the direction of the proton beam. For these measurements, the neutron beam to the counter was defined by a collimator having a slit $1\frac{1}{4}$ in. high and $\frac{1}{4}$ in.[3] wide. Many narrow levels were further studied by use of an entrance slit $\frac{1}{8}$ in. wide. The entrance to the collimator was placed 13 in. from the neutron source. Because of the presence of so many peaks between 350 and 500 kev, this region was re-investigated by self-detection. For these self-detection measurements and for all measurements above 500 kev, neutrons emitted in the direction of the proton beam were used for the following reasons: (1) The higher counting rates obtainable are especially needed for self-detection measurements; (2) up to about 640 kev,[5] the beam of neutrons at 0° is free of the second group of low-energy neutrons that arises from the formation of the residual nucleus Be^7 in the 430-kev state; and (3) neutrons of a given energy are produced at a lower accelerator voltage at 0° than at large angles of emission; so the deuterons contaminating the proton beam are less energetic, and, therefore add fewer and less energetic neutrons to the background. On the other hand, one is beset with a larger neutron energy spread because, for a given lithium target, the neutron energy spread at 0° is approximately twice that at 120°. This, however, is offset to some degree by the fact that the neutron energy is almost independent of angle near 0° but is strongly dependent at 120°. For all measurements at 0°, the entrance aperture of the collimator through which the neutrons reached the detector had a diameter of 0.3 in. and was located about 11 in. from the source of neutrons. All self-detection measurements were made by use of a sodium metal scattering sample 800 mils thick placed in the neutron counter (see Fig. 1 of reference 3). Flat-detection measurements were made by use of a Lucite scattering sample 6 in. long. Above about 400 kev, a graphite scattering sample 6 in. long was used. Transmission samples of different thicknesses were used to maintain a transmission of 50% to 60%.

During these measurements, lithium targets ranging from 0.6–0.8 kev in thickness (determined by the rise-

* For preliminary results of these measurements on Na^{24}, see C. T. Hibdon, Bull. Am. Phys. Soc. 4, 404 (1959); **5**, 295 (1960).

† Work performed under the auspices of the U. S. Atomic Energy Commission.

[1] C. T. Hibdon, Phys. Rev. **118**, 514 (1960).
[2] P. H. Stelson and W. M. Preston, Phys. Rev. **88**, 1354 (1952).
[3] C. T. Hibdon, Phys. Rev. **108**, 414 (1957).
[4] C. T. Hibdon, Phys. Rev. **114**, 179 (1959).
[5] A. S. Langsdorf, Jr., J. E. Monahan, and W. A. Reardon, Argonne National Laboratory Topical Rept. ANL-5219, Argonne, Illinois, 1954 (unpublished); A. B. Smith (private communication).

curve method[6]) were used. Each day a target of lithium metal was evaporated in vacuum onto the 10-mil tantalum end cap of the rotating target assembly.[3] [*Note added in proof.* This target is cooled by a blast of air. The backing does not contribute appreciably to the background, as shown by the fact that the background does not change as the threshold of the reaction is crossed.] The voltage scale of the generator is based on the $Li^7(p,n)$ threshold which is taken to be 1.882 Mev. Daily calibrations for the series of targets were almost identical. The energy spread of the neutrons was estimated by the rise-curve method outlined in reference 3; but this is done at threshold and the spread is known to increase with neutron energy. Therefore, the over-all resolution is unknown in the region under study, and no level is sufficiently narrow and well isolated to be used in measuring the spread. However, the degree to which the many overlapping and interfering levels are resolved indicates that the spread in neutron energy is not excessive. Some narrow levels were resolved to considerably higher peak values (and the valleys between them were deeper) by self-detection than by flat detection. This effect is evident for such peaks as Nos. 70, 72, 77, 78, 80, 85, 96, 98, 121, and 133. This indicates that their true widths must be near or less than the over-all neutron energy spread. The overlapping wings of other neighboring levels prevent a detailed study of any of these levels to obtain an estimate of the over-all neutron energy spread; but the degree to which these levels are resolved indicates that the effective spread in neutron energy is less than one kev for self-detection measurements.

The data shown in the various figures are the raw data with no corrections applied other than background[3] and small normalizations to the monitor (long counter). The monitor was placed about 50 in. from the lithium target in the direction of the proton beam when measurements were made at 120°, and about 30° from the direction of the proton beam when the measurements were made at 0°. [*Note added in proof.* The method of determining the background is described on p. 415 of reference 2 and was found to be unaffected by the presence of the wheels carrying the samples.]

The in-scattering of neutrons by the sodium samples and their containers was investigated for 625-kev neutrons. Figure 1 shows the results obtained for three different samples of sodium. The relative counting rates, corrected for background, are shown for various positions of these samples. Since these curves are horizontal straight lines, no change occurs in the in-scattering and one may place the samples at any point shown in Fig. 1. The points represented by crosses indicate the positions at which the samples were placed for neutron cross-section measurements. No corrections were applied for in-scattering nor for multiple scattering.

[6] A. O. Hanson, R. F. Taschek, and J. H. Williams, Revs. Modern Phys. **21**, 635 (1949).

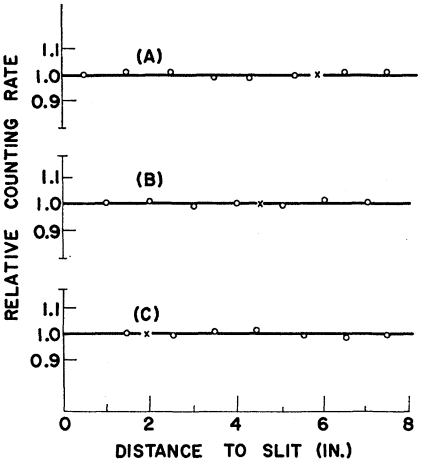

FIG. 1. In-scattering of 625-kev neutrons by sodium samples and containers. Sample thickness: (A) 1.00 in., (B) 2.00 in., and (C) 3.00 in. The crosses indicate the positions of samples for neutron cross-section measurements. Statistical errors are approximately the diameters of the circles.

3. EXPERIMENTAL RESULTS

The observed neutron total-cross-section data from 350 to about 630 kev are shown in Figs. 3, 5, 7, 10, 11, and 13. Open circles are used to indicate the points obtained by flat detection and solid circles the points obtained by self-detection. In this region 71 peaks were observed and, when combined with the previous data[1] up to 350 kev, this brings the total to 157 peaks in the region from about 1 to 630 kev for an average level spacing of approximately 4 kev for all levels. An examination of the data shows that many features in the data[1] below 350 kev appear to continue in this region. Variations in the cross section show that a complicated level structure for Na^{24} continues on up to 630 kev. Because of the observable features of the data, one expects a profusion of p-, d-, and f-wave levels ($l=1, 2, 3$) in this region and an assortment of values for the angular momentum J. Relatively few of the peaks appear to be s wave ($l=0$), identifiable by their asymmetrical shapes and the presence of deep minima on their low-energy sides. It is of particular interest to note that the very wide peaks observed by Stelson and Preston[2] are clusters of peaks. (1) The large peak observed by them just below 400 kev is composed of many peaks. A number of these in the region from about 385–405 kev appear to have high values of J. (2) The large peak near 450 kev consists of two peaks with others in their wings. (3) The very wide s-wave peak near 540 kev is an s-wave level (No. 114) but is much narrower than the value given by Stelson and Preston. A cluster of peaks (Nos. 111, 112, and 113) is located near its minimum and a multitude of peaks exist in its high-energy wing. (4) A large peak near 600 kev persists but many smaller peaks are present in both wings.

It is desirable to know whether a general missing of levels begins in the high-energy region and, if so, to

what extent the levels are missed. A knowledge of the distribution of the level spacings, whether the levels occur at random or at regular intervals, is also of interest both for practical purposes and for a comparison with the theory of nuclear structure. Figure 2 shows a plot of the distribution of the levels in which the number of levels with energies $\leq E_n$ is plotted as a function of the neutron energy E_n for all levels up to 630 kev. This distribution exhibits the following characteristics: (1) There is no downward curvature to indicate a general missing of levels in the high-energy region; (2) the observed levels are spaced somewhat at random—not at equal intervals; (3) the plot does, however, show a general trend toward a linear distribution, the fluctuations about this line presumably resulting in part from irregularities introduced by missing some levels too narrow to be resolved. In addition, the element of randomness in level spacings expected from any appropriate model of the nucleus would introduce irregularities in the distribution. One should then expect the plot to show some deviations from a linear distribution.

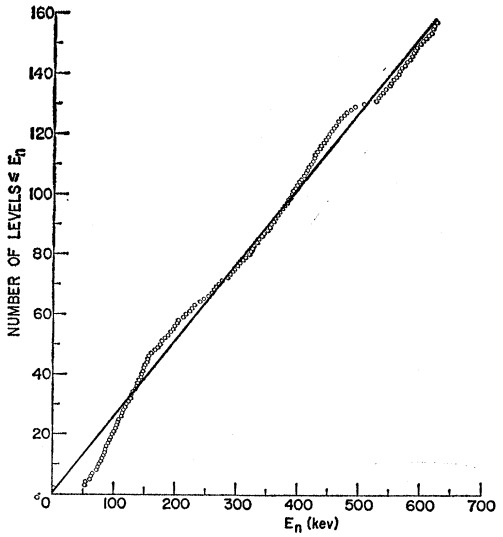

FIG. 2. Number of levels of Na^{24} with energies $\leq E_n$ as a function of the neutron energy E_n.

4. ANALYSES OF THE RESONANCE LEVELS

A. Preliminary Topics

Certain limitations are inherent in the determination of the parameters of the levels. Values assigned to these parameters depend on the degree to which the levels were resolved. The density of levels is so great that one must try to take account of the many overlapping and interfering wings of the levels. No level can be treated as a well-isolated level. The interaction of the neutrons with the nuclei are taken to be predominantly elastic scattering. However, in the presence of other processes, such as (n,p), (n,α), (n,γ), or inelastic scattering, only lower limits can be placed on the values of J. Because of their large negative Q values,[2] the (n,p) and (n,α) reactions cannot occur in this energy range. Recent measurements of the (n,γ) process by Cubitt and Bame[7] show broad maxima near 300 and 600 kev. Each maximum exhibits a peak height of less than a millibarn, so this process can also be omitted in the present analyses. Inelastic scattering is not completely negligible but measurements[8] of this cross section up to an energy above 800 kev show peaks beginning at 482 kev, but no peak has a cross section above about 240 millibarns. It then appears that the resonances of sodium in this energy region may be treated as elastic scattering resonances.

[7] S. J. Bame and R. L. Cubitt, Phys. Rev. **113**, 256 (1959).

[8] H. J. Hausman, J. E. Monahan, F. P. Mooring, and S. Raboy, Bull. Am. Phys. Soc. **1**, 56 (1956); J. E. Monahan, F. P. Mooring, and S. Raboy, Argonne National Laboratory Rept. ANL-5609, Argonne, Illinois, 1956 (unpublished), p. 106; and private communication.

B. Potential Scattering σ_p and the Method of Analysis

A value of the potential scattering σ_p that is reasonably close to its true value must be determined before an analysis of the levels can be performed. However, σ_p cannot be determined directly from the data since none are free of contributions from the wings of one or more levels. The depth of the minimum of the large s-wave level No. 114, if known, would provide an excellent and most straightforward method of determining a fairly unambiguous value of σ_p because the value of J is easily shown to be 2 for this level; but the depth of the minimum of this level cannot be determined because of the presence of peaks Nos. 111, 112, and 113 at or near this minimum. The region between 490 and 530 kev does exhibit the least number of levels, but the low-energy wing of the large s-wave level No. 114 extends into and beyond this region and, therefore, depresses the cross section everywhere in this region. On the other hand, the wings of other levels also extend into this region and offset this depression to some extent. There is no other region so free of levels and, therefore, the best indication of σ_p comes from this region and indicates a value in the neighborhood of 2 barns, which is close to the theoretical value obtained from $\sigma_p = \sum_l (2l+1) 4\pi \lambda\!\!\!^{-2} \sin^2\delta_l$, where $\delta_0 = R/\lambda\!\!\!^{-}$ and $R = r_0 A^{\frac{1}{3}}$. The value of r_0 is assumed to be 0.14×10^{-12} cm. In the region below 350 kev, it was found that the theoretical value of σ_p appeared to be as good a value as one could expect.[1] It will also be assumed for the present analyses.

The method of analysis is the same as that used for the region below 350 kev.[1] For some levels, estimated parameters were used to obtain single-level plots which approximately fit the data. The parameters were then

repeatedly revised until a best fit was obtained. By a "peeling-off" process the analyses could then be continued. Because of the density of levels, this process proved to be successful in only a limited number of cases. Sometimes the plots of several levels considered simultaneously provided better fits for the data. Many multiple-level plots were necessary, and finally, for most groups of levels, a combination of single-level plots for some levels and multiple-level plots for others turned out to be a better approach. Many repetitions in the analyses are avoidable by first removing the extensive wings of recognizable s-wave levels. If, in the course of analysis, additional s-wave levels are detected, these levels are combined with other s-wave levels for a final check. Then pertinent analyses up to that point are repeated. Assignments were made to the highest values of J that are consistent with the data. Fortunately, the many tedious calculations needed were performed by the Applied Mathematics Division on the IBM-704 and GEORGE computers. [*Note added in proof.* The tabulated values of Γ_n and E_r in Table I are the values for which the computer program gave a best fit to the experimental points, the best fit being determined by visual comparison. The equations on which the program is based are given in reference 4, p. 182 where Eq. (3) is used for single-level plots and Eq. (2) for multiple-level plots. The variation of the width Γ_n with energy is included in accordance with $\Gamma_n=2P_l\gamma_l^2$ so that the wings of the levels may be extended as far as needed. The quantity P_l is the penetrability factor given by $P_0=x$, $P_1=x^3/(x^2+1)$, etc., with $x=R/\lambda$. Considerable thought has been given the problem of correlating the two types of data obtained by flat- and self-detection and the neutron energy spread in an effort to obtain an analytical method for determining the correct value of J for narrow levels. This method is quite involved and when completed will constitute a separate paper. However, in its approximate form, applicable only at the peaks of levels, it has been applied to the narrow levels in the present work and agrees with the J-value assignments. In applying the method, corrections were made for the wings of nearby levels.]

TABLE I. Summary of the levels of Na^{24} (from 350–630 kev) derived from neutron reactions with Na^{23}. The parameters J, Γ_n, and l are probable values obtained as a best fit to the data. The sample thickness used for self-detection measurements at the peaks of the resonances is given by N_s. The sample thickness for flat detection is the same as N_s for the wide resonances and up to 50% more for the narrow ones.

No.	E_r (kev)	J	l	Γ_n (kev)	N_s (10^{24} atoms/cm^2)	No.	E_r (kev)	J	l	Γ_n (kev)	N_s (10^{24} atoms/cm^2)
68	352.6	1	1	1.6	0.127	104	465.7	2	0	0.70	0.127
69	355.9	1	1	1.5	0.127	105	471.5	2	3(2)	0.70	0.127
70	359.7	2	2	0.9	0.127	106	476.5	2	2	1.3	0.127
71	362.0	2	2	1.0	0.127	107	481.3	2	3(2)	0.75	0.127
72	363.8	2	2	0.8	0.127	108	487.2	2	3	1.1	0.127
73	368.0	1	1	1.6	0.127	109	493.9	2	3	0.75	0.127
74	372.2	2	1	0.9	0.127	110	511.0	2	3	1.0	0.127
75	375.0	2	1	1.5	0.127	111	530.3	3	3	0.75	0.127
76	378.9	2	1	1.6	0.095	112	532.7	3	3	1.0	0.127
77	382.7	3	3(2)	0.9	0.095	113	535.4	3	3	1.1	0.127
78	384.7	2	1	1.5	0.095	114	538.8	2	0	4.5	0.127
79	388.8	3	3(2)	1.4	0.064	115	545.0	2	3	0.6	0.127
80	391.2	3	3(2)	0.7	0.064	116	549.9	2	2	1.4	0.095
81	393.6	3	3(2)	0.8	0.064	117	552.8	2	2	1.4	0.127
82	397.9	4	2	1.3	0.064	118	557.0	3	3(2)	0.8	0.095
83	400.5	4	2	1.4	0.095	119	561.2	3	2(3)	1.3	0.095
84	403.0	4	2(3)	1.1	0.095	120	564.8	3	2(3)	1.3	0.095
85	405.8	2	0	3.0	0.095	121	568.3	3	3(2)	0.6	0.127
86	411.2	2	2	1.5	0.095	122	570.4	3	3(2)	0.9	0.127
87	414.6	3	3(2)	0.9	0.095	123	575.3	3	2	1.5	0.095
88	417.0	2	3(2)	1.2	0.127	124	578.7	2	2	2.0	0.127
89	419.1	3	3(2)	0.9	0.127	125	582.9	3	2(3)	1.6	0.127
90	421.6	2	0	1.9	0.127	126	586.6	3	2(3)	1.6	0.095
91	426.5	1	3(2)	0.9	0.127	126A	590.0	1	2	1.6	
92	428.4	2	3	0.6	0.127	127	592.8	4	3	1.2	0.095
93	430.4	2	3	0.7	0.127	128	595.3	4	3	1.3	0.095
94	432.2	2	3	0.9	0.127	129	601.0	4	2	3.5	0.076
95	436.5	3	3	0.7	0.127	130	605.0	3	3	1.7	0.095
96	439.0	3	3(2)	1.1	0.127	131	608.3	4	3	1.0	0.095
97	443.0	3	2(3)	1.3	0.127	132	611.3	3	3	1.7	0.095
98	446.2	4	3(2)	1.2	0.095	133	615.2	4	3	1.1	0.095
99	449.6	4	2(3)	1.9	0.064	134	618.8	3	3	1.7	0.095
100	451.2	2	0	3.7	0.095	135	621.0	4	3	0.8	0.095
101	456.6	2	3(2)	0.8	0.095	136	623.0	4	3	0.8	0.095
102	459.7	2	3(2)	0.6	0.127	137	626.2	3	2	2.7	0.095
103	463.2	2	2(3)	1.1	0.127						

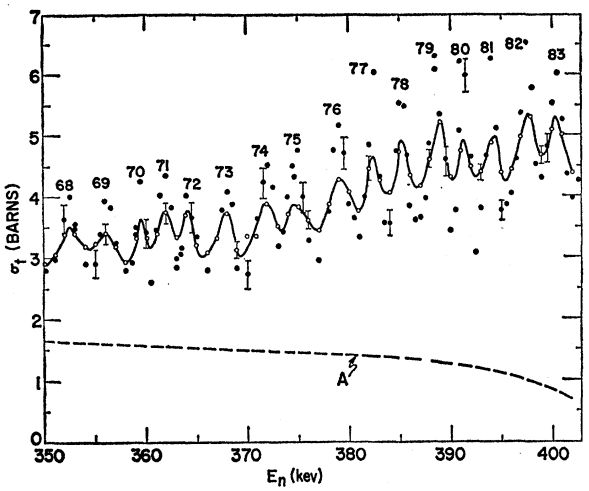

FIG. 3. Neutron total cross section of sodium from 350–400 kev. Open circles show data obtained by flat detection; solid circles data by self-detection. Curve (A) is a multiple-level plot of the s-wave levels that extend into this region. It includes the potential scattering.

C. Analyses of the s-Wave Levels

An analysis of a group of levels without regard for the influence of the wings of levels in other groups may lead to erroneous results. The wings of wide levels, particularly s-wave levels, often extend into the region of other groups of levels and appreciably elevate or depress the cross section in an entire region. In the present data a few peaks, such as Nos. 85, 90, 100, 104, and 114, appear to be s-wave levels with a value of $J=2$. Peak No. 114 is due to a relatively wide level and, therefore, its wings are expected to extend to large distances. The wings of this level combined with the wings of the other s-wave levels may, then, extend into most of the regions of concern here. Further, the combined configuration of peaks Nos. 99 and 100 indicate that these peaks are attributable to a p- (or d-) and an s-wave level, respectively, because they exhibit a shape very similar to that of peaks Nos. 42 and 43, which have already been analyzed (see Fig. 15 of reference 1). Peak No. 99, is, then, located near the minimum of No. 100. The relative positions of No. 99 and the minimum of No. 100 are such as to produce a distortion in the shape of 99. This distortion is clearly recognizable in Fig. 7. A provisional set of parameters for these two levels revealed that it is necessary to include the multiple-level plot of all pertinent s-wave levels along with the plots of other neighboring levels. The plot of the s-wave levels that provides the best fit is shown by curve (A) in Figs. 3, 5, 8, 10, 11, and 13. This curve is a combination of the potential scattering and the multiple-level plot of all of the s-wave levels from 300–630 kev. The level parameters of the various s-wave levels used to obtain this plot are listed in Table I of this paper and in Table I of reference 1.

D. Analyses of the Resonance Levels from 350–445 kev

In this region, many peaks of various heights and generally narrow widths were observed during measurements by flat detection. These data are shown in Figs. 3 and 5 by open circles and were obtained by use of neutrons emitted at an angle of 120° with respect to the direction of the proton beam. Because of the narrow widths of these levels and the large level density, each level was restudied by self-detection. For this study, neutrons emitted in the direction of the proton beam were used to obtain a higher counting rate. These data are represented by solid circles in Figs. 3 and 5 and, for many of the levels, the peaks were much better resolved (with poorer statistics) than they were by flat detection. The highest peaks cluster in the region around 390–400 kev and, along with neighboring peaks, account for the large peak observed near 395 kev by Stelson and Preston.[2] By subtracting curve (A) (potential scattering plus the wings of s-wave levels) from the data, one obtains the curves shown in Figs. 4 and 6. These curves, then, represent the only resonance contributions of the levels in this region. The loci of the single-level theoretical peak heights for $J=1$, 2, 3, and 4 are also included.

Consider first the region from 350 to 405 kev, which is shown in Figs. 4 and 6. Apparently no s-wave levels are present in this region, since there are no clearly defined dips on the low-energy sides of the peaks and no peak appears to be clearly asymmetrical in shape. The solid curve, then, is composed of the resonance contributions of the many p- and d- (and possible f-) wave levels. There does not appear to be any way to begin a "peeling-off" process among this maze of levels,

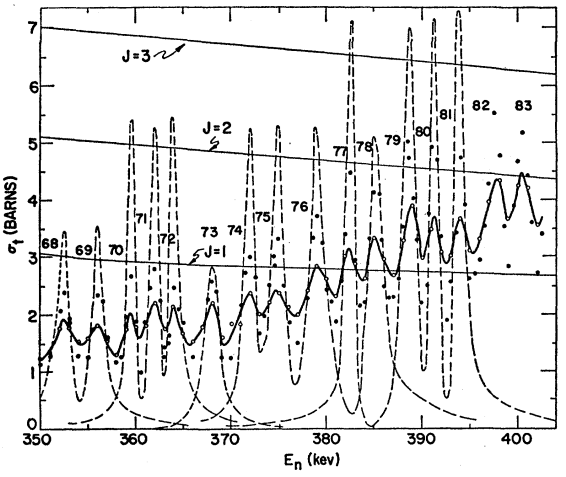

FIG. 4. Analyses of the levels of Na^{24} from 350–395 kev. The points shown were obtained by subtracting curve (A) in Fig. 3 from the data. The dashed curves are the theoretical plots obtained by use of the resonance parameters listed in Table I. The lines showing possible peak heights for $J=1$, 2, and 3 are for single-level peak heights and do not include the potential scattering.

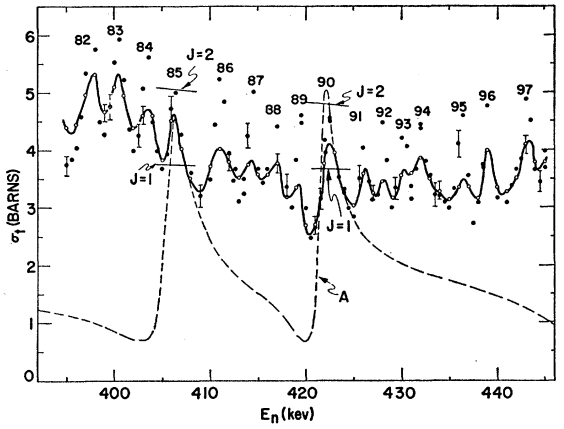

FIG. 5. Neutron total cross section of sodium from 395–445 kev. Open circles show data obtained by flat detection; solid circles data by self-detection. Curve (A) is a multiple-level plot of the *s*-wave levels that extend into this region and the *s*-wave resonance levels Nos. 85 and 90. It includes the potential scattering.

and one must then resort to a trial and error process. The apparent relative widths of the peaks, their relative heights, and the depths of the minima between peaks, however, do indicate the following: (a) peaks Nos. 68, 69, and 73 appear to be attributable to $J=1$; (b) peaks Nos. 70, 71, 72, 74, 75, 76, and 78 to $J=2$; and (c) peaks Nos. 77, 79, 80, and 81, to $J=3$. The peak heights of the last four definitely rule out a value of $J=2$ and the depths of the minima near 390 and 393 kev indicate mutual interference. The depths of the minima near 399 and 402 kev also indicate mutual interference

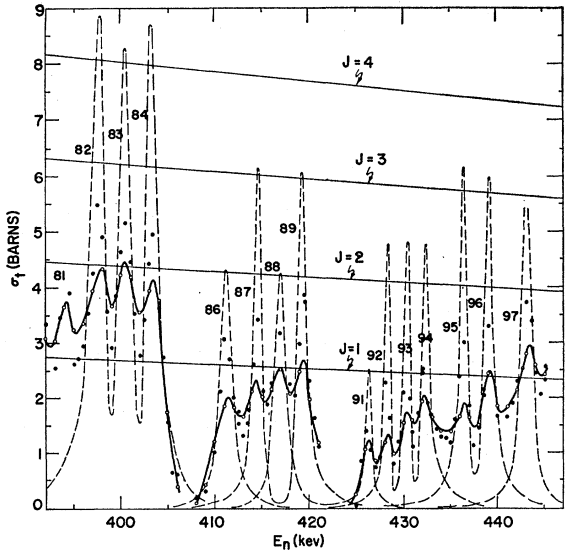

FIG. 6. Analyses of the levels of Na^{24} from 395–445 kev. The points shown were obtained by subtracting curve (A) in Fig. 5 from the data. The various curves shown by broken lines are the theoretical plots for the best fits obtained. The lines showing the possible single-level peak heights for J from 1 to 4 do not include the potential scattering.

among peaks Nos. 82, 83, and 84 (Fig 6). The depth of the minimum between Nos. 81 and 82 and the spacing of nearly 4 kev indicate that mutual interference does not occur between these two levels. Therefore, the value of J is taken to be 4 for each of the peaks Nos. 82, 83, and 84. The reduced widths favor the values of l that are listed in Table I. The parameters of the various levels were adjusted repeatedly until the plots shown by broken lines in Figs. 4 and 6 were obtained.

Two peaks (Nos. 85 and 90) of the remainder up to 445 kev have already been assigned to *s*-wave levels (Fig. 5) with a value of $J=2$. Curve (A) in Fig. 5 shows a multiple-level plot of these and other *s*-wave levels above 300 kev. By subtracting this curve from the data, one obtains the curves shown in Fig. 6. In the region from about 410 to 420 kev, four peaks are present. The

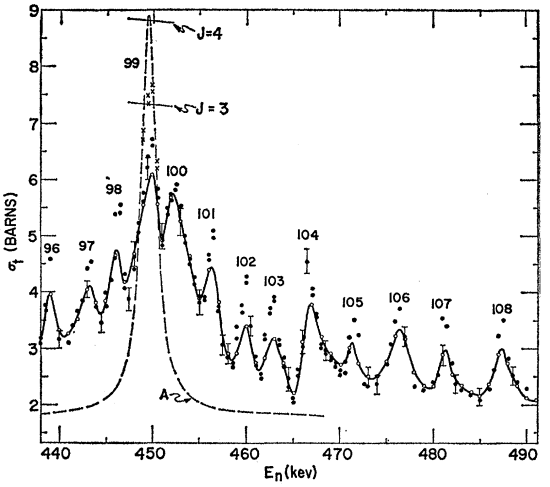

FIG. 7. Neutron total cross section of sodium from 440–490 kev. Open circles show data obtained by flat detection; solid circles data by self-detection. Curve (A) is a single-level plot (including potential scattering) for resonance level No. 99. Points shown by crosses were obtained by making corrections to the self-detection data because of the minimum of the *s*-wave resonance No. 100.

self-detection data definitely rule out a value of $J=1$ for all of these four peaks. Because of their relative widths, the value of J is taken to be 2 for Nos. 86 and 88 with $l=2$ and 3, respectively. Resonances Nos. 87 and 89 are apparently narrower than Nos. 86 and 88 and their peaks are higher. The value of J is then taken to be 3 with $l=3$ for these two peaks. It appears that peak No. 91 is attributable to an *f*-wave level with a value of $J=1$ and Nos. 92, 93, and 94 to *f*-wave levels with a value of $J=2$. Moreover, the depths of the various minima indicate mutual interference for Nos. 92, 93, and 94. The peak heights of Nos. 95, 96, and 97 are too high for a value of $J=2$ for levels of these apparent widths. The value of J is, then, taken to be 3 for each of these peaks. The depth of the minimum between Nos. 95 and 96 indicates mutual interference between this pair of levels. The spacing between Nos. 96 and 97 is great enough that a deep minimum be-

tween these peaks would have been observed if it existed. Since none was observed, the value of l for No. 97 differs from the value for the other two levels. The width of No. 97 appears to be larger than the width of either of the other two levels. Therefore, the value of l is taken to be 2 for No. 97 and 3 for each of the other two. The curves shown by broken lines in Fig. 6 appear to provide the best fit for these levels. The parameters used to obtain these curves are shown in Table I.

E. Analyses of the Resonance Levels from 445–480 kev

The data for this region are shown in Fig. 7. From a casual examination of these data, one expects peaks Nos. 100 and 104 to be due to s-wave levels. The minimum of No. 100 appears to be located just below the peak of No. 99. The peak and low-energy wing of No. 99 are depressed to such an extent that the distortion in the shape of this peak is clearly discernible in Fig. 7. The self-detection and flat-detection data both show this distortion. It was found by trial and error that a more direct approach to the analysis was to include the single-level plot of No. 99 with the plot of the s-wave levels. When the parameters of these levels are found, the various levels can then be "peeled-off" by beginning with No. 99. By subtracting the single-level plot of No. 99 [curve (A) in Fig. 7] from the data, one obtains the two parts of curve (B) in Fig. 8. In Fig. 8 the multiple-level plot of the s-wave levels is shown by curve (A). Only the resonance contributions are represented by this curve, because the potential scattering was included in curve (A) in Fig. 7. By subtracting curve (A) from curve (B) in Fig. 8, one obtains the three parts of curve (A) in Fig. 9. The observed peak heights of these d- and f-wave levels are reduced by the neutron energy spread which is expected to increase with energy. This was taken into account in assigning values of J. The various plots, obtained by use of the parameters listed in Table I, are shown by dashed curves in Fig. 9.

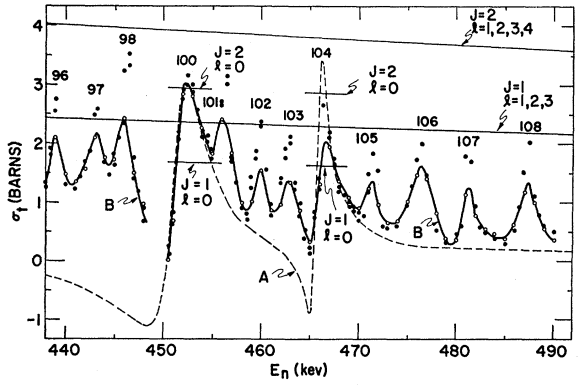

FIG. 8. Analyses of the levels of Na^{24} from 440–490 kev. The points shown were obtained by subtracting curve (A) in Fig. 7 from the data. Curve A in Fig. 8 shows the multiple-level plot of the s-wave levels. The potential scattering is not included in any of these curves.

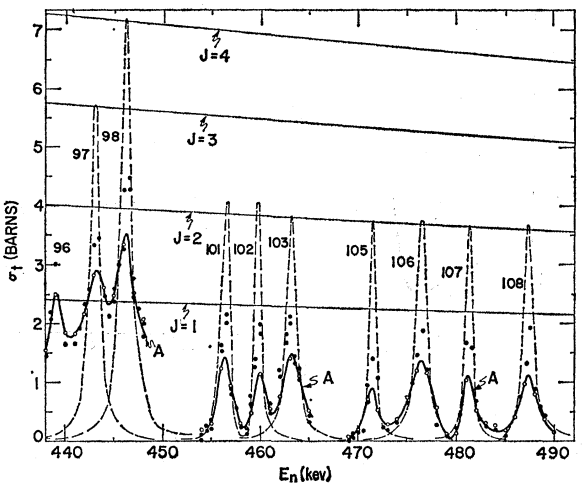

FIG. 9. A continuation of the analyses of the levels of Na^{24} from 440–490 kev. The points shown were obtained by the subtractions shown in Figs. 7 and 8. The dashed single- and multiple-level plots show the best fits for the resonance levels. The loci of the theoretical single-level peak heights are shown for various values of J. The potential scattering is not included in any of these curves.

F. Analyses of the Resonance Levels from 480–525 kev

The data in this region are shown in Fig. 10. Only a small number of levels occur in this region and, because of their narrow widths, they are attributable to f-wave levels. Curve (A) shows the multiple-level plot of the wings of s-wave levels located in other regions,

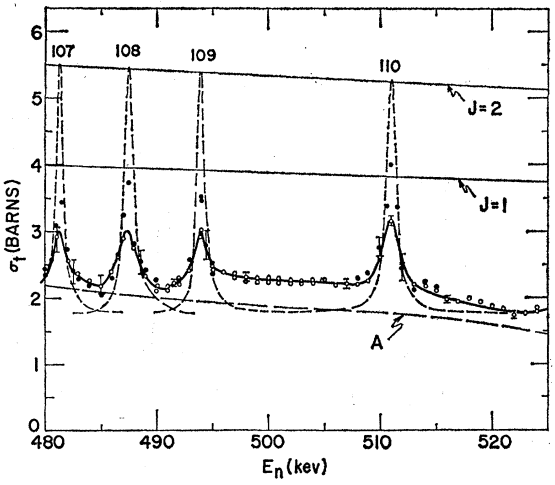

FIG. 10. Neutron total cross section of sodium from 480–525 kev. Open circles show data obtained by flat detection; solid circles data by self-detection. Curve (A) is a multiple-level plot of the s-wave levels. The dashed curves show the analyses of the levels.

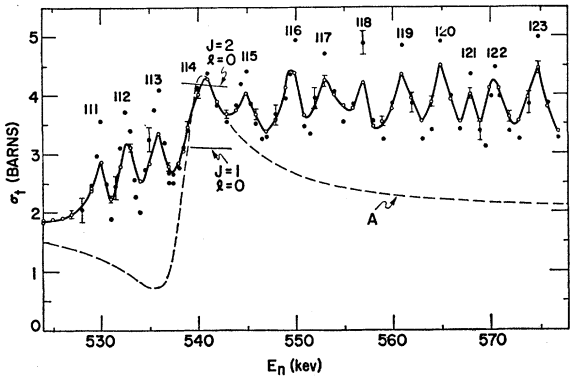

FIG. 11. Neutron total cross section of sodium from 525–577 kev. The self-detection data are shown by solid circles; flat-detection data by open circles. Curve (A) shows the multiple-level plot of the *s*-wave levels.

No. 114 being the nearest one. The plots shown by dashed curves were obtained by use of the parameters listed in Table I. Because of the relatively large level spacings, only single-level plots are shown.

G. Analyses of the Resonance Levels from 525–577 kev

The data for this region are shown in Fig. 11. One large *s*-wave level, peak No. 114, is the predominant one. The analysis of this level has already been given and the multiple-level plot is shown by curve (A). By subtracting this curve from the data one obtains the two parts of curve (A) in Fig. 12. Because of the neutron energy spread and the relative widths and heights of the peaks in Fig. 12, the value of J is taken to be 3 for Nos. 111, 112, and 113. An *f*-wave multiple-level plot is shown in Fig. 12 for the widths listed in Table I. The value of J is taken to be 2 for peaks Nos. 115, 116, and 117 and 3 for the remainder of the peaks in this region. A larger value of l is expected for No. 115 than for Nos. 116 and 117 for two reasons: (a) The width of No. 115 is much smaller than the widths of the other two; and (b) the depth and shape of the wide minimum between Nos. 115 and 116 do not indicate mutual interference between this pair of levels. The widths of the levels appear to be too small for *p*-wave levels in this region. Therefore, the value of l is taken to be 3 for No. 115 and 2 for Nos. 116 and 117. The plots shown by dashed lines in Fig. 12 appear to agree with these assignments. Because of the depths of the various minima and apparent widths of the remainder of the levels in this region, the value of l is taken to be 3 for Nos. 118, 121, and 122 and 2 for the others. The various single- and multiple-level plots for these levels are shown by dashed curves in Fig. 12 and appear to agree with the assignments.

H. Analyses of the Resonance Levels from 577–630 kev

No peak in this group (Fig. 13) appears to exhibit a pronounced dip on its low-energy side nor the asymmetrical shape characteristic of an *s*-wave level. One, then, concludes that all of these levels are attributable to *d*- or *f*-wave levels. The high-energy wing of the *s*-wave level, peak No. 114, does, however, extend into this region and provides a background upon which the group sits. This background includes the potential scattering and is represented by curve (A) in Fig. 13. It is convenient to begin the analyses of this group with peak No. 129 because it is apparently the widest one and its wings are sufficiently well defined to obtain a width of 3.5 kev for a value of $J=4$. The single-level plot for $l=2$ is shown by curve (B) in Fig. 13. By subtracting curve (A) [and that part of curve (B) due to the resonance contribution of peak No. 129] from the data, one obtains the two parts of curve (A) in Fig. 14.

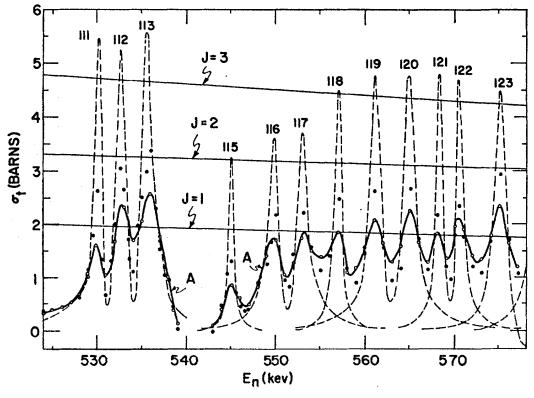

FIG. 12. Analyses of the levels of Na^{24} from 525–577 kev. The points shown were obtained by subtracting curve (A) in Fig. 11 from the data. The dashed single- and multiple-level plots show the best fits for the resonance levels. The lines showing the possible peak heights for the various values of J represent single-level heights. The potential scattering is not included in any of these curves.

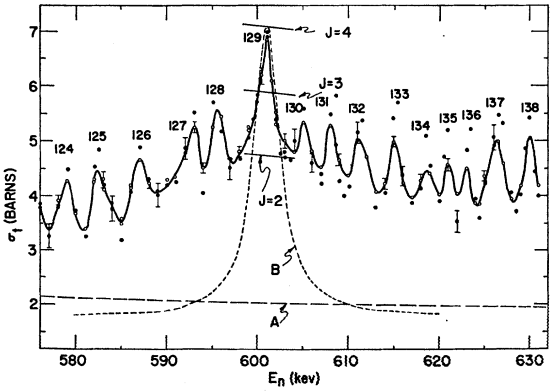

FIG. 13. Neutron total cross section of sodium from 576–630 kev. Solid circles show the data obtained by self-detection; open circles the data by flat detection. Curve (A) is a multiple-level plot of the *s*-wave levels plus the potential scattering. Curve (B) is a single-level plot of the *d*-wave level No. 129 plus the potential scattering.

Figure 14 is, then, divided into two groups. In the first group up to 600 kev, the following assignments were made: (a) $J=2(l=2)$ for No. 124; (b) $J=3(l=2)$ for Nos. 125 and 126; and (c) $J=4(l=3)$ for Nos. 127 and 128. The widths were determined by trial and error. Except for the region between peaks Nos. 126 and 127, the various plots shown by dashed curves in Fig. 14 appear to agree with the assignments. The multiple-level plot for Nos. 125 and 126 also includes No. 123. Between Nos. 126 and 127, the data indicate the presence of an unresolved peak. By subtracting the multiple-level plots from the data, one obtains the points represented by crosses. The dashed curve for $J=1$, $l=2$ and $\Gamma_n=1.6$ kev appears to agree with this small peak No. 126A.

Above 600 kev the level structure is somewhat more complicated but the data do provide some helpful aids. (a) The low-energy wing of peak No. 130 is well defined and from this wing a width of 1.7 kev was estimated for $J=3$ and $l=3$. (b) The peak heights and relative widths indicate a value of $J=4$ for Nos. 131, 133, 135, and 136 and a value of $l=3$. The widths were determined by trial and error and are tabulated in Table I. (c) The widths of Nos. 132 and 134 are wider and the value of J is taken to be 3 with $l=3$ and each has a width of 1.7 kev. (d) The single-level plot for No. 137 was obtained for $J=3$, $l=2$ and $\Gamma_n=2.7$ kev.

Table I shows a summary of the parameters of the 71 levels in this region. Table II shows the number of levels assigned to each value of J and their distribution among the various values of J. All of the levels of Na^{24} up to 630 kev are included (see the earlier report[1] for the levels up to 350 kev). This distribution and the values of Γ and l for the various levels are only as valid as the analyses. The parameters listed in Table I are those that appear to give a best fit to the data.

There appear to be no really definite characteristics or rules that distinguish clearly between values of l for $l>0$. A comparison of the measured reduced neutron width γ^2 with the Wigner limit,[9,10] $\hbar^2/(\mu R^2)\approx 2.45$ Mev for Na^{24}, may be used as a rough guide. However, in the present analyses this rough guide provides little real help, because the neutron widths of the levels for $l=1$, 2, or 3 are much less than the Wigner limit. The

TABLE II. The number of levels and their distribution among the various values of the angular momentum J. The relative numbers are the ratios of the densities of levels to the density for $J=1$. All resonance levels of Na^{24} up to 630 kev are included.

J	0	1	2	3	4
Number of levels	27	47	45	26	12
Relative numbers	0.57	1	0.96	0.55	0.26

[9] C. E. Porter and R. G. Thomas, Phys. Rev. **104**, 483 (1956).

[10] R. G. Thomas, Phys. Rev. **97**, 224 (1955). The upper limit on γ^2 is given by $\hbar^2/(\mu R^2)\approx 40/R^2$, where R is expressed in units of 10^{-13} cm and for Na^{24} the limit is about 2.45 Mev.

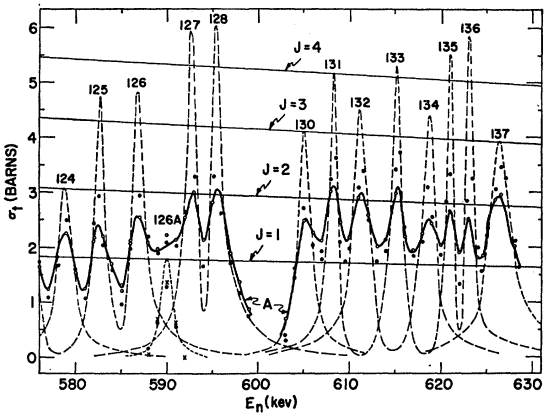

FIG. 14. Analyses of the levels of Na^{24} from 576–630 kev. Points shown were obtained by subtracting curve (A) and the resonance component of curve (B) in Fig. 13 from the data. The dashed single- and multiple-level plots show the best fits for the resonance levels. Peak No. 126A "peeled-off" during the analyses.

various peak heights, widths of levels, and depths of neighboring minima provide strong arguments for the presence of values of $l=1$, 2, and 3. To analyze the data one, then, must assign various values of l that will allow or exclude mutual interference. On this basis the assignments show the ratio of odd to even parities to be about 3 to 2.

5. DISTRIBUTION OF THE ANGULAR MOMENTA AMONG THE NUCLEAR LEVELS

For the single-particle model, Bloch gives the density of levels as a function of the total angular momentum J by the expression[11]

$$\rho(U,J) = \rho(U)\{\exp[-J^2/2\sigma^2]-\exp[-(J+1)^2/2\sigma^2]\}, \quad (1)$$

where $\rho(U,J)$ is the density of all levels for the energy region in question and U is the excitation energy. The quantity $2\sigma^2$ is given by some authors as $2c\tau$ or $a\tau$, where τ is the so-called nuclear temperature. Equation (1) can be used to compute the ratios of the densities of levels for different values of J to the density for $J=1$. Plots of these ratios for three values of σ are shown in Fig. 15. The experimental data for the relative numbers in Table II are shown in the plot by solid circles and for comparison the data for Al^{28} are shown by open circles. For Na^{24}, these data indicate a value of $\sigma=1.8$.

For the constant a in the relation $2\sigma^2=a\tau$, Cameron[12] gives the expression

$$a=0.1181A^{5/3}[1+3.0052/A^{2/3}-4.0298/A^{4/3}], \quad (2)$$

[11] C. Bloch, Phys. Rev. **93**, 1094 (1954). See also H. A. Bethe, Revs. Modern Phys. **9**, 69 (1937), formula (301); J. M. B. Lang and K. J. LeCouteur, Proc. Phys. Soc. (London) **A67**, 586 (1954); T. D. Newton, Can. J. Phys. **34**, 804 (1956). Note also that the expression for $\rho(U,J)$ is often written in the approximate form $\rho(U)[(2J+1)/2\sigma^2]\exp[-(J+\frac{1}{2})^2/2\sigma^2]$.

[12] A. G. W. Cameron, Can. J. Phys. **37**, 244 (1959).

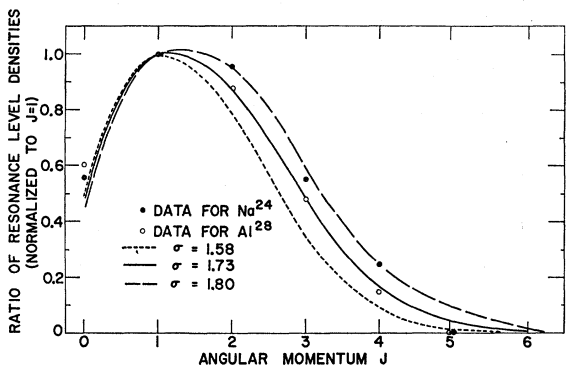

FIG. 15. Distribution of the angular momenta among the resonance levels of Na^{24}. Experimentally determined points are shown by solid circles. The experimental points for Al^{28} are shown by open circles (see reference 4). The curves are plots of Eq. (1) for values of $\sigma=1.58$, 1.73, and 1.80.

which for Na^{24} is 3.2. This leads to $\tau\approx 2$ Mev, which is close to the value[4] found for Al^{28}.

The level density $\rho(U)$ is given by Bloch[11] in the form

$$\rho(U)=[U(96\pi)^{\frac{1}{2}}]^{-1}\exp[\pi(2U/3\delta)^{\frac{1}{2}}], \qquad (3)$$

where δ is the average level spacing of the nucleons in the nucleus. From the present measurements, the experimentally determined density of all levels is $\rho(U)=239$ Mev^{-1}. For a mean value of $U=7.3$ Mev and the value of $\sigma=1.8$ obtained from the distribution of the angular momenta, one obtains a value of $\delta=0.40$ Mev compared with an expected theoretical value[13] of about 0.50 Mev.

6. DISTRIBUTION IN THE SIZE OF THE NEUTRON WIDTHS

The reduced widths obtained from the neutron widths of the levels by the relation[4] $\gamma^2=\Gamma_n/(2P_l)$ were found to fluctuate violently among the levels of Na^{24} in a manner similar to the fluctuations of the reduced widths[4] of Al^{28}. It is expected that the reduced widths will obey the Porter-Thomas[9] distribution $x^{-\frac{1}{2}}(\exp-x/2)$ or possibly an exponential distribution e^{-x}, where the quantity $x=\gamma^2/\langle\gamma^2\rangle_{av}$ is evaluated for a given J and parity and γ^2 and $\langle\gamma^2\rangle_{av}$ refer to a particular J and parity. In Fig. 16 the number of levels per interval Δx is plotted as a function of x for the present data for all of the levels of Na^{24} up to 630 kev. The straight line shown in the figure is an exponential plot drawn for $c=120$, where c is the value of the proportionality constant in the equation $y=c\exp(-x)$ and y is the number of levels per interval Δx. Figure 17 shows a plot of the same data for a Porter-Thomas distribution. The present data, then, appear to agree equally well with the exponential and Porter-Thomas distributions. It is important in nuclear theory and to nuclear engineering to know which of the two distributions, the one given by Porter and Thomas[9] or the simpler exponential one, is more likely to be correct. Theoretical analyses[9] show that the Porter-Thomas distribution is more reasonable on theoretical grounds and assign to the exponential distribution a small probability of being the correct one. A more accurate evaluation of the parameters of the levels may indicate a preference for one of the distributions.

7. DISTRIBUTION OF THE LEVEL SPACINGS

The fluctuation of individual level spacings relative to the mean has received considerable attention during recent years. (See reference 4 for a list of references to the original papers.) The simplest assumption, namely that levels occur completely at random, would lead to an exponential distribution

$$N=k\exp(-s), \qquad (4)$$

where $s=S/D$. The quantity S represents the individual level spacing and D the average level spacing. The quantity N is the number of spacings per unit interval Δs and k the total number of spacings. However, it was pointed out by Wigner[4] that, if one assumes a random distribution of the Hamiltonian matrix elements, then the levels of the same spin and parity repel each other.

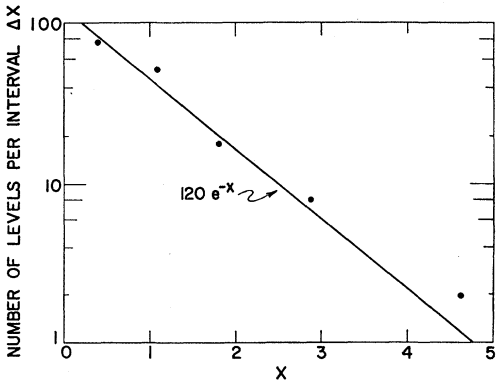

FIG. 16. Exponential distribution of the reduced neutron widths of Na^{24}.

[13] A. A. Ross, Phys. Rev. **108**, 720 (1957).

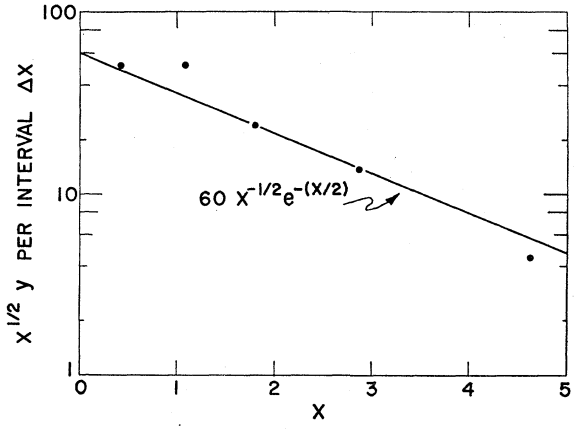

FIG. 17. Porter-Thomas distribution of the reduced neutron widths of Na^{24}.

For small values of S, the distribution should be proportional to SdS. Wigner surmised that the complete distribution would be given approximately by the expression

$$N=k\pi(S/2)\exp(-\pi S^2/4). \quad (5)$$

In an attempt to see the level repulsion, the observed levels were separated into sequences, each belonging to a given spin and parity, and the mean spacing was computed separately for each sequence. The several distributions thus obtained were then combined into a single group in order to reduce statistical fluctuations. Figure 18 shows a plot of the number of spacings per interval $\Delta S=0.5$ as a function of S for all of the levels of Na^{24} up to 630 kev. Solid circles represent the data and are located at the midpoints of the respective intervals. For comparison, the theoretical distributions given by Eqs. (4) and (5) are also shown in Fig. 18. The data are in closer agreement with the exponential distribution than the Wigner surmise. Although the experimental distribution appears not to agree with the Wigner surmise, it should be noted that some levels very likely have been missed and the parameters of some levels misassigned. Such errors would tend to distort the correct distribution into one similar to an exponential distribution.

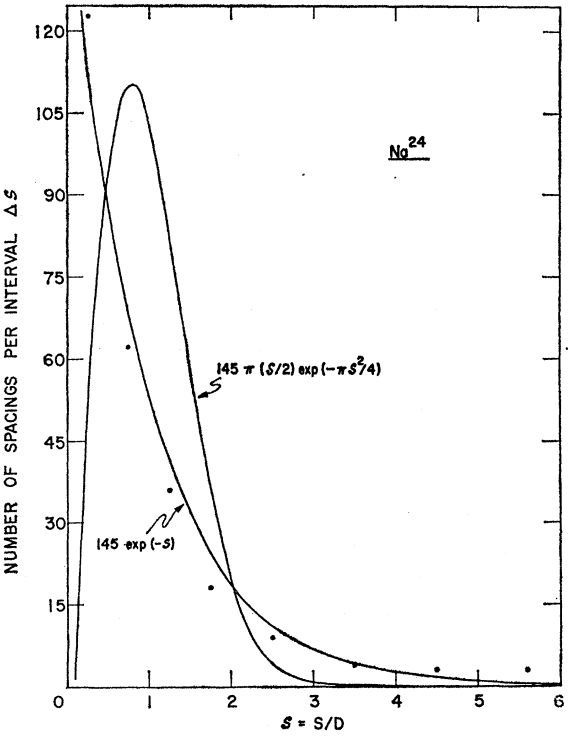

FIG. 18. Distribution of the level spacings of Na^{24}.

8. STRENGTH FUNCTIONS

The strength function is given by the expression $\langle\gamma^2\rangle_{av}/D$, the ratio[4] of the average reduced neutron width to the average level spacing where the reduced neutron width $\gamma^2=\Gamma_n/(2P_l)$ and the level spacing are averaged for a given value of l. For the s-wave levels in the present data, the strength function averaged over both values of J is 0.045; and averaged over all values of J for the p-wave levels it is 0.37, which is approximately eight times as large as for the s-wave levels. These results agree with the model of Feshbach, Porter, and Weisskopf[14] who predict a p-wave maximum near $A=25$ and a low value for s-wave levels for a nuclear well depth of 40 Mev. Moreover, the sum rule of Lane, Thomas, and Wigner[15] suggests that the sum of the reduced widths of a given group of levels in an energy interval comparable with the spacings of giant resonances for a given value of l should not exceed $\hbar^2/(\mu R^2)$. For the p-wave levels in the present measurements, this sum is 0.38 of the Wigner limit and further indicates that this interval of energy is near the maximum for the strength function for $l=1$. Further, it should be noted that the strength function for the levels assigned to d-wave neutron interactions in the present measurements is 4.7 and that the sum of the reduced neutron widths far exceeds the Wigner limit. This value of the strength function, is then, about 100 times the value for s-wave levels, although the two values might be expected to be of the same order of magnitude since the levels are of even parity. It was also found that the strength function for the f-wave levels is about 15, which is many times as large as the value for the p-wave levels. The strength function for the f-wave levels might be expected to show a peak near the peak of the p-wave levels but it should not be expected to exceed it by so large a factor. The large values for the d- and f-wave strength functions undoubtedly are attributable to one or more of the following factors: (a) the assignment of too many levels to values of $l=2$ and 3; (b) a possible error in the expression for the penetrability factors P_2 and P_3; or (c) a strong dependence of the reduced neutron width on l. The levels in this region are certainly expected to be composed of a number of d- and f-wave levels, so a very large error in the assignments would be necessary to account for the large values of the strength functions.

9. DISTRIBUTION OF THE EXCITED NUCLEAR LEVELS

Figure 2 shows a plot of the virtual nuclear levels of Na^{24} with energies $\leq E_n$ as a function of the neutron energy E_n, but it is not known whether or not this curve would join on smoothly with a similar plot of the bound levels. Presumably, all of the bound levels have not been resolved and a discontinuity would be expected in the curve if the distribution shown in Fig. 2

[14] H. Feshbach, C. E. Porter, and V. F. Weisskopf, Phys. Rev. 96, 448 (1954).
[15] A. M. Lane, R. G. Thomas, and E. P. Wigner, Phys. Rev. 98, 693 (1955).

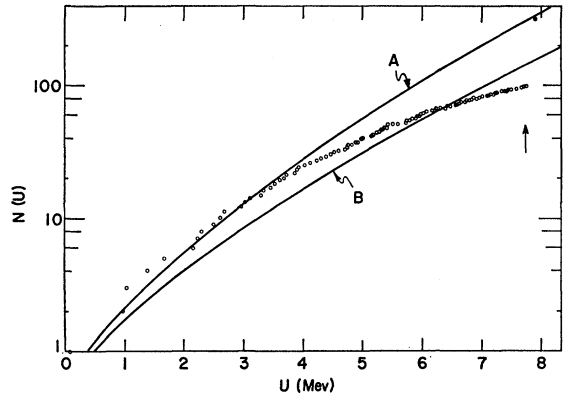

FIG. 19. Distribution of the nuclear energy levels of Al^{28}. Curve (A) was obtained from Eq. (7) (times a factor of 1.8) for a value of $\delta=0.50$ Mev and curve (B) for $\delta=0.60$ Mev. The arrow indicates the binding energy, 7.723 Mev.

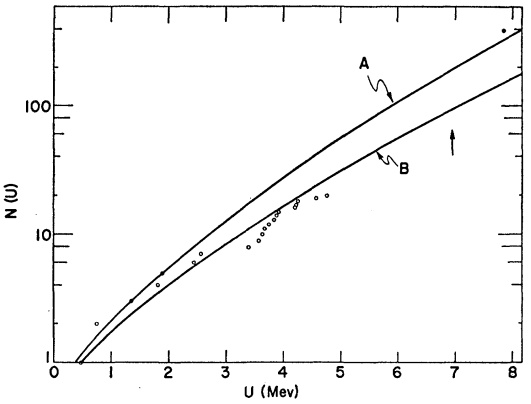

FIG. 20. Distribution of the nuclear energy levels of Na^{24}. Curve (A) was obtained from Eq. (7) (times a factor of 1.8) for a value of $\delta=0.50$ Mev and curve (B) for $\delta=0.60$ Mev. The arrow indicates the binding energy, 6.956 Mev.

included the bound levels. Then, in order to relate the number of virtual levels to the number of bound levels, one needs an expression for the total number of levels up to a given excitation energy U. The total number of levels in the energy interval from U_1 to U_2 is given by the expression

$$N(U)=\int\rho(U)dU, \tag{6}$$

where $\rho(U)$ is the density of all levels in the energy interval. The theoretical number of levels, then, depends on the form of $\rho(U)$. It is well known that $\rho(U)$ has an essentially exponential behavior and a number of expressions have been given for it. Here, the expression given by Bloch, Eq. (2) of the present paper, will be used. The integral, Eq. (6), then reduces to the form

$$N(U)=2C\left[\ln x+ax+\frac{a^2x^2}{2\times2!}+\frac{a^3x^3}{3\times3!}+\cdots\right], \tag{7}$$

where $x=U^{\frac{1}{2}}$, $C=[\sigma(96\pi)^{\frac{1}{2}}]^{-1}$, and $a=\pi[2/(3\delta)]^{\frac{1}{2}}$. The number of levels up to the excitation energy U, then, depends on the constant σ, which is proportional to the nuclear temperature (assumed to be constant for each nucleus), and on δ, the average level spacing of the individual nucleons in the nucleus. Because of the first term in Eq. (7), the summation over the levels cannot begin with the ground level, whose excitation energy is $U=0$, but instead must begin with some excited level. It was found that for a value of $\delta=0.50$ Mev and a value of U as low as 0.10 kev, the value of N from Eq. (7) is a small negative number. By making this small correction for the lower limit, Eq. (7) should then reflect the distribution of all of the nuclear levels above the ground level for the proper values of δ and σ. If all of the bound levels of a nucleus were known up to say 5 Mev, a family of curves obtained from Eq. (7) would indicate the proper values of σ and δ for each nucleus. Apparently, the number of levels that have been resolved for any one nucleus is insufficient for an evaluation of σ and δ, but approximate values of these two constants for Na^{24} and Al^{28} have been determined from the distribution of the angular momenta.

Only about 20 of the bound levels[16] of Na^{24} appear to have been resolved and this is really too few to be of much use for this purpose. However, approximately 100 bound levels[17] are known for Al^{28}. This is the largest number of bound levels known for any odd-odd nucleus in this region and is therefore the most suitable nucleus for a check of Eq. (7). Figure 19 shows the number of bound levels of Al^{28} plotted against U, which is expressed in the center-of-mass system. A plot of Eq. (7) for values of δ of 0.50 or 0.60 Mev falls below the plot of the bound levels of Al^{28} and plots for smaller values of δ show steeper curves. It was found that a reasonable fit to the data, up to about 4 Mev, for $\delta=0.50$ Mev occurs if Eq. (7) is multiplied by the constant 1.8. This plot is shown by curve (A) in Fig. 19. A similar plot is shown by curve (B) for $\delta=0.60$ Mev. If curve (A) represents the correct distribution, it is evident that many of the bound levels above 4 Mev are still unresolved. Erickson[17] has shown that the number of levels up to an excitation energy U is the product of the nuclear temperature τ and the density of levels, $N(U)=\tau\rho(U)$. By use of this relation, the point shown by a solid circle in Fig. 19 was obtained from the neutron resonances.[4] This, then, suggests that the distribution of the nuclear levels is given by some such curve as (A) in Fig. 19. Figure 20 shows a similar plot of the 20 nuclear levels of Na^{24}. The trend of the levels up to about 2.5 Mev indicates that a value of 0.50 Mev for δ may also be about right for Na^{24}. The value of $N(U)$ calculated from Erickson's expression[17] from the level density of the neutron resonances and the nuclear

[16] P. M. Endt and C. M. Braams, Revs. Modern Phys. **29**, 683 (1957).
[17] T. Erickson, Nuclear Phys. **11**, 481 (1959).

temperature is shown by the solid circle in Fig. 20 and seems to further indicate that the value of δ is about 0.50 Mev. This value of $N(U)$ is somewhat above curve (A), but it is believed that the value of the nuclear temperature used is too large.

Presumably, it may be too stringent a requirement to expect a plot (such as Figs. 19 and 20) of the first few nuclear levels of a nucleus to obey Eq. (7). However, plots have been made for the known levels of many nuclei and they all show that curves similar to the ones shown in Figs. 19 and 20 are followed surprisingly well. Families of curves were also plotted for a few values of δ. From these plots and the curves for various values of δ (not shown) a number of other trends were observed: (a) The larger values of δ are associated with nuclei which have small nuclear level densities. (b) The value of δ appears to be large for light nuclei (there being fewer levels for these nuclei) and decreases as one goes to heavier nuclei but shows peaks in the neighborhood of magic numbers and then decreases sharply again above these numbers. The value of δ appears to be the largest for even-even nuclei. (c) The distribution of the levels of the even-even nuclei may be given by Eq. (7) for a suitable choice of δ and of σ without multiplying the equation by a constant factor. If a multiplicative constant is needed, it is probably less than unity. (d) The distribution of the levels of the odd-even and even-odd nuclei apparently can be given by Eq. (7) if σ and δ are suitably chosen. (e) For the odd-odd levels, apparently Eq. (7) must be multiplied by a constant of the order of the value of σ. A more detailed study on the basis of the presently known levels is expected to confirm these trends. The larger values of δ for the lighter nuclei seem to agree with the trend for the theoretical values.[14] The influence of the shell structure on the level density of a highly excited nucleus has been studied theoretically by Rosenzweig.[18] This study indicates trends similar to the ones stated above, particularly the trend noted in (b).

10. DISCUSSION

The results show that the large level density of Na^{24} continues on up as far as the present measurements were made. The large levels previously reported in this region by Stelson and Preston[2] were found to be composed of many levels. This accounts for the large widths which these experimenters reported for these levels. The large s-wave level near 540 kev reported by these authors was confirmed to be an s-wave level having a value of $J=2$ but it has a width of only 4.5 kev. It is the widest s-wave level found in Na^{24} and is the widest level in the region from 350 to 630 kev. A number of narrow levels occur in or near the minimum of this s-wave level and many levels occur in its high-energy wing. Because of the profusion of levels with narrow widths, all of the levels in this region were studied by self-detection in order to determine better values of the parameters of the levels. The various figures show the highest peak values obtained and the lowest minima between peaks. No really good value of the neutron energy spread could be obtained because no well-isolated narrow level occurred to enable one to study the energy spread of the neutrons. However, as discussed in Sec. 2, some fair estimates could be made and these estimates indicate that the energy spread is about 1 kev or a little less for the lithium targets used. Consequently, only a few of the levels were resolved to peak heights very near their true values. Because of this, the parameters determined for many of the levels may differ somewhat from their true values and this in turn would produce irregularities in the distribution of the angular momenta, level spacings, and neutron widths. However, since no really serious irregularities occurred in these distributions, the parameters of most of the levels are probably reasonably close to their true values.

Values of the strength functions obtained for the s- and p-wave levels are comparable[4] with those obtained for Al^{28} and are in accord with the predictions of the theory.[14] The unusually high values for d- and f-wave levels were discussed in Sec. 8.

The potential scattering was assumed to be given by the expression

$$\sigma_p=\sum_l (2l+1)4\pi\lambda\!\!\!^{-2} \sin^2\delta_l,$$

for reasons given in Sec. 4(B). This value was also used in the analyses of the levels in the energy region up to 350 kev. The results obtained in all of the analyses up to 630 kev indicate that this value of the potential scattering must be near the true value.

The material included in Sec. 9 indicates that a much higher percentage of the virtual levels are being resolved by the present techniques than are resolved in the region of the bound levels. Previously, it was not known whether or not the neutron energy spread in this energy region might possibly preclude the resolution of levels as narrow as the ones observed. Also, it was not known if the shielding of the counting equipment was sufficient to maintain an acceptable background. By making measurements with neutrons at 0° with respect to the direction of the proton beam and using thin lithium targets, one can, as the present results show, resolve (at least partially) many narrow levels. The background was found to be quite small as compared with the counting rate. Lately, it has also been found that measurements can be extended to even higher energies.

The differential neutron cross-section measurements made by Lane and Monahan[19] in the vicinity of the

[18] N. Rosenzweig, Phys. Rev. **108**, 817 (1957).

[19] R. O. Lane and J. E. Monahan, Phys. Rev. **118**, 533 (1960).

large peaks of Na^{24} reported by Stelson and Preston[2] indicate: (a) appreciable interference of levels of opposite parity; (b) the presence of s-wave levels in the region around 400 kev; (c) a dominant s-wave dependence near 450 kev; and (d) a strong s-wave level around 540 kev. The present data together with the results obtained by the analyses are consistent with these indications. Each large level reported by Stelson and Preston[2] was found to consist of a number of levels of opposite parity. Two s-wave levels do occur near 400 kev and the dominant level near 450 kev appears to be an s-wave level. The widest s-wave level found in Na^{24} is located near 540 kev.

ACKNOWLEDGMENTS

I wish to express my appreciation to Dr. F. E. Throw for his comments and suggestions with the manuscript, and to Dr. J. E. Monahan and Dr. Norbert Rosenzweig for their suggestions concerning the sections on strength functions and the distribution of the levels. I also wish to gratefully acknowledge the assistance of Jack Wallace, William Evans, and the Van de Graaff crew consisting of Walter Ray, Jr., Ronald Amrein, Robert Kickert, John Bicek, Robert Peterson, Joseph Ragusa, and Peter J. Billquist for their aid in making the measurements. I wish also to thank the Applied Mathematics Division for much of the detailed computations.

PHYSICAL REVIEW VOLUME 122, NUMBER 4 MAY 15, 1861

Reduced Widths and Isotopic Spin Impurities of $\frac{1}{2}+$ States of N^{15}†

J. B. FRENCH*
Sarah Mellon Scaife Radiation Laboratory, University of Pittsburgh, Pittsburgh, Pennsylvania, and Fysisch Laboratorium der Rijksuniversiteit, Utrecht, The Netherlands

SYUREI IWAO‡
University of Rochester, Rochester, New York

AND

ERICH VOGT§
Atomic Energy of Canada Limited, Chalk River, Ontario, Canada

(Received January 3, 1961)

The nuclear reactions $C^{14}(p,n)N^{14}$ and $C^{14}(p,\gamma_0)N^{15}$, for protons of less than 1.6 Mev involve the interference of two adjacent states having the same spin and parity ($\frac{1}{2}+$) but different isotopic spin ($T=\frac{1}{2}$ and $\frac{3}{2}$). By taking properly into account the effect of other, more distant $\frac{1}{2}+$ levels on the cross section near the interfering pair of levels, we are able to fit well the (p,n) cross section from the neutron threshold up to a proton energy of 1.6 Mev and to obtain reliable estimates for the reduced width amplitudes of the interfering pair, as well as for the physically significant phases of the amplitudes. Since the neutron decay of the $T=\frac{3}{2}$ state is "forbidden," the neutron reduced widths of the close-lying pair lead to a direct measure 4% of the isotopic spin impurity of the pair. The results found in the cross section analysis are compared to shell model calculations based on the N^{15} wave functions of Halbert and French, and reasonably satisfactory agreement is found.

I. INTRODUCTION

THE nuclear reactions $C^{14}(p,n)N^{14}$ and $C^{14}(p,\gamma_0)N^{15}$, for proton energies of less than 1.6 Mev, have several unusual features of importance for nuclear structure. The (p,n) reaction cross section has been measured at several laboratories[1–3] while the (p,γ_0) results are given by Bartholomew *et al.*[1] The $C^{14}+p$ cross sections are shown on Fig. 1 along with a diagram of the levels of N^{15} which lie at or near the energy reached by $C^{14}+p$. The information on the compound states of N^{15} has been found from a variety of reactions as summarized by Ajzenberg-Selove and Lauritsen.[4] Although we shall consider the effects due to other states in describing the $C^{14}(p,n)N^{14}$ reaction, our interest will focus on the two adjacent $\frac{1}{2}+$ states at excitation energies of 11.438 and 11.610 Mev in N^{15}. These states are known to have isotopic spin $T=\frac{1}{2}$ and $T=\frac{3}{2}$, respectively.[5] The latter level is therefore forbidden to decay to the ground state of N^{14} by neutron emission.

As we shall see below, the two adjacent $\frac{1}{2}+$ states

† Supported in part by the U. S. Atomic Energy Commission and by Atomic Energy of Canada Limited.

* On leave from the University of Rochester, National Science Foundation Senior Postdoctoral Fellow at Utrecht, 1959–1960.

‡ Present address: Physics Department, University of Syracuse, Syracuse, New York.

§ This work was begun while E. Vogt was visiting the Physics Department of the University of Rochester, 1958–1959.

[1] G. A. Bartholomew, F. Brown, H. E. Gove, A. E. Litherland, and E. B. Paul, Can. J. Phys. **33**, 441 (1955).

[2] R. M. Sanders, Phys. Rev. **104**, 1434 (1956).

[3] J. H. Gibbons and R. L. Macklin, Phys. Rev. **114**, 571 (1959). The authors are grateful to Dr. Gibbons and Dr. Macklin for sending their results before publication.

[4] F. Ajzenberg-Selove and T. Lauritsen, Nuclear Phys. **11**, 1 (1959).

[5] G. A. Bartholomew, A. E. Litherland, E. B. Paul, and H. E. Gove, Can. J. Phys. **34**, 147 (1956).